Original Article | Neuroimaging and Head & Neck

eISSN 2005-8330
https://doi.org/10.3348/kjr.2021.0603
Korean J Radiol 2022;23(2):237-245

Korean Journal of Radiology
KJR

Quantification of Nerve Viscosity Using Shear Wave Dispersion Imaging in Diabetic Rats: A Novel Technique for Evaluating Diabetic Neuropathy

Feifei Liu*, Diancheng Li*, Yuwei Xin, Fang Liu, Wenxue Li, Jiaan Zhu

All authors: Department of Ultrasound, Peking University People's Hospital, Beijing, China

Objective: Viscoelasticity is an essential feature of nerves, although little is known about their viscous properties. The discovery of shear wave dispersion (SWD) imaging has presented a new approach for the non-invasive evaluation of tissue viscosity. The present study investigated the feasibility of using SWD imaging to evaluate diabetic neuropathy using the sciatic nerve in a diabetic rat model.

Materials and Methods: This study included 11 diabetic rats in the diabetic group and 12 healthy rats in the control group. Bilateral sciatic nerves were evaluated 3 months after treatment with streptozotocin. We measured the nerve cross-sectional area (CSA), nerve stiffness using shear wave elastography (SWE), and nerve viscosity using SWD imaging. The motor nerve conduction velocity (MNCV) was also measured. These four indicators and the histology of the sciatic nerves were then compared between the two groups. The performance of CSA, SWE, and SWD imaging in distinguishing the two groups was assessed using receiver operating characteristic (ROC) analysis.

Results: Nerve CSA, stiffness, and viscosity in the diabetic group was significantly higher than those in the control group (all $p < 0.05$). The results also revealed a significantly lower MNCV in the diabetic group ($p = 0.005$). Additionally, the density of myelinated fibers was significantly lower in the diabetic group ($p = 0.004$). The average thickness of the myelin sheath was also lower in the diabetic group ($p = 0.012$). The area under the ROC curve for distinguishing the diabetic neuropathy group from the control group was 0.876 for SWD imaging, which was significantly greater than 0.677 for CSA ($p = 0.030$) and 0.705 for SWE ($p = 0.035$).

Conclusion: Sciatic nerve viscosity measured using SWD imaging was significantly higher in diabetic rats. The viscosity measured using SWD imaging performed well in distinguishing the diabetic neuropathy group from the control group. Therefore, SWD imaging may be a promising method for the evaluation of diabetic neuropathy.

Keywords: *Diabetic neuropathy; Shear wave elastography; Shear wave dispersion; Sciatic nerve*

INTRODUCTION

Diabetic peripheral neuropathy (DPN) is one of the most common and serious complications of diabetes mellitus (DM), affecting up to 50% of patients with DM [1,2]. This condition results in various complications, such as sensory and motor dysfunction, lower limb reinfection, ulcers, and amputation, leading to severe disability, decreased quality of life, and even death [3,4]. Given the high incidence of DPN and the serious consequences of the relevant complications, early diagnosis and treatment are important. However, it is still difficult to diagnose DPN in its early stages [5].

Electrophysiological examination can detect DPN and is currently considered the gold standard for diagnosis. However, this procedure is time-consuming and painful for patients. Additionally, small and unmyelinated fibers are preferentially affected in the early stages of DPN.

Received: May 17, 2021 **Revised:** October 8, 2021
Accepted: October 23, 2021
*These authors contributed equally to this work.
Corresponding author: Jiaan Zhu, MD, PhD, Department of Ultrasound, Peking University People's Hospital, No. 11 Xizhimen South Street, Xicheng District, Beijing 100044, China.
• E-mail: zhujiaan@pkuph.edu.cn

Nonetheless, electrophysiological examinations have poor sensitivity in detecting changes in these fibers [5]. Previous studies also showed that most electrophysiological results are generally normal in patients with small fiber neuropathy [6,7]. Moreover, a clinico-electrophysiological dissociation phenomenon frequently occurs in the early stages of DPN [8], which might lead to missed or late diagnosis of the condition.

Shear wave elastography (SWE) is a noninvasive evaluation technique that can reveal the elasticity of tissues through the propagation of shear waves. Additionally, previous studies that used SWE to evaluate nerve entrapment or DPN reported that the technique could detect an increase in nerve stiffness. In addition, nerve stiffness measured using SWE could better diagnose DPN than cross-sectional area (CSA) [9,10]. However, the clinical value of SWE in the early detection of DPN remains debatable. This is because previous research showed that there was no significant difference in nerve stiffness, measured using SWE, between patients with DM without clinical or electrophysiological signs of DPN and healthy controls [11,12].

The ultrasound (US) elastography models currently used in clinical practice are assumed to be linear, isotropic, and homogeneous. In addition, only the elasticity of tissues is quantified, and tissue viscosity is often neglected. Existing evidence also suggests that dispersion is related to the frequency dependence of both the speed and attenuation of shear waves in the viscous component. Additionally, both the shear wave speed and attenuation are more pronounced with increasing frequency. Therefore, tissue viscosity can be measured indirectly through the analysis of shear wave dispersion (SWD) [13]. Currently, SWD imaging, which can measure tissue viscoelasticity, has been used in clinical practice, and the results have shown that viscosity may be related to steatosis, necrosis, and inflammation [14-17]. Viscoelasticity is an essential feature of biological tissues, including nerves that possess both viscous and elastic properties [18]. Furthermore, it was confirmed that microvascular abnormalities and inflammation are involved in the pathogenesis of DPN [19-21]. Therefore, the viscosity of nerves may be an important index for the detection of DPN. However, to date, no study has used SWD imaging to detect changes in the viscosity of peripheral nerves in DM.

Consequently, the present study hypothesized that the pathophysiological features of DPN affect the viscosity of nerves, which can be assessed using SWD imaging. Notably, pathological changes are required to verify the feasibility of viscosity, which can be measured using SWD imaging, in the diagnosis of DPN. However, it is difficult to assess human nerves, and nerve biopsy is an invasive and highly specialized procedure [2]. Therefore, the present study aimed to investigate the feasibility of using SWD imaging to evaluate diabetic neuropathy using the sciatic nerve in a streptozotocin (STZ)-induced diabetic rat model.

MATERIALS AND METHODS

Establishment of a Model for Diabetic Rats

A total of 27 male Sprague-Dawley (SD) rats (Beijing Vital River Laboratory Animal Technologies Co. Ltd.) aged 8 weeks and weighing 250–300 g were used in this study. All SD rats were acclimatized in a specific pathogen-free experimental environment for 7 days. The control group rats (n = 12) were fed an ordinary diet without any treatment. We followed the protocol established by Reed et al. [22] to develop type 2 DM. Fifteen rats were fed a high-glucose high-fat diet for 2 weeks and then administered a single intraperitoneal injection of 50 mg/kg STZ (Sigma Chemical Co.). Seven days after treatment with STZ, 11 rats with random blood glucose concentrations higher than 16.7 mmoL/L were assigned to the diabetic group (n = 11); four rats were excluded because their blood glucose level was lower than 16.7 mmoL/L [23]. The success rate of DM modelling was 73.3%. The bilateral sciatic nerves were evaluated using SWD imaging 3 months after treatment with STZ. All experimental procedures involving animals were approved by the Institutional Animal Care and Use Committee of Peking University People's Hospital (IRB No. 2017PHC061).

Ultrasound Examination

All US examinations were performed using an 18-MHz linear-array transducer (Aplio i800, Canon Medical Systems). In addition, the rats were anesthetized using an intraperitoneal injection of ketamine/xylazine mix (60 mg/kg ketamine, 7.5 mg/kg xylazine). The SD rats were laid in the lateral position, with their hind limbs relaxed.

SWD imaging was performed with care to avoid the compression effect of the transducer. After acquisition of the shear wave propagation data, the US system automatically displayed the twin view of grayscale images and shear wave propagation maps, and then switched to the quad-view mode including four maps (namely, the

https://doi.org/10.3348/kjr.2021.0603

Korean Journal of Radiology
KJR

elasticity map, shear wave propagation map, grayscale image, and SWD map) after 5 seconds of cooling (Fig. 1). Under the guidance of the propagation map, the region of interest (ROI) was placed to correspond with the smooth and parallel lines on the propagation map, indicating stable measurement conditions. Additionally, the activation of shear wave propagation and data filling of the sample box were performed five times for each nerve.

Moreover, CSA and SWD/SWE were measured by tracing directly over the epineurium of the sciatic nerve in the transverse plane at the level of the greater trochanter of the femur. The SWD and SWE of nerves were measured five times at each site from five independent images to increase reproducibility, with the average value being chosen for subsequent analysis. If distorted or not parallel shear wave propagation was observed or there was color drop-out in the ROIs, SWD was considered a technical failure [16-18]. In addition, all SWE and SWD measurements were independently taken by two operators, with more than 10 years of experience in US and 5 years of experience in elastographic studies. Furthermore, operator 2 was blinded to the results obtained by Operator 1. Operator 1 repeated the operations 30 minutes after the initial examinations.

Electrophysiological Studies

The rats were anesthetized using a ketamine/xylazine mix through an intraperitoneal injection (60 mg/kg ketamine, 7.5 mg/kg xylazine). Thereafter, the motor nerve conduction velocity (MNCV) of the sciatic nerve was measured using a TECA Synergy electronic medical instrument (VIASYS Healthcare), in both the diabetic and control groups. The stimulating electrode was placed on the proximal and distal sides of the compression area of the sciatic nerve (stimulation duration, 0.1 ms; frequency, 1 Hz; stimulus intensity, 0.12 mA). Additionally, the reference recording electrode was inserted into the quadriceps femoris, while the recording electrode was placed on the tibialis anterior muscle.

Histological and Quantitative Morphometry of the Sciatic Nerve

The rats were euthanized using an overdose of pentobarbital (75 mg/kg, i.p.), after which the bilateral sciatic nerves were isolated and harvested from

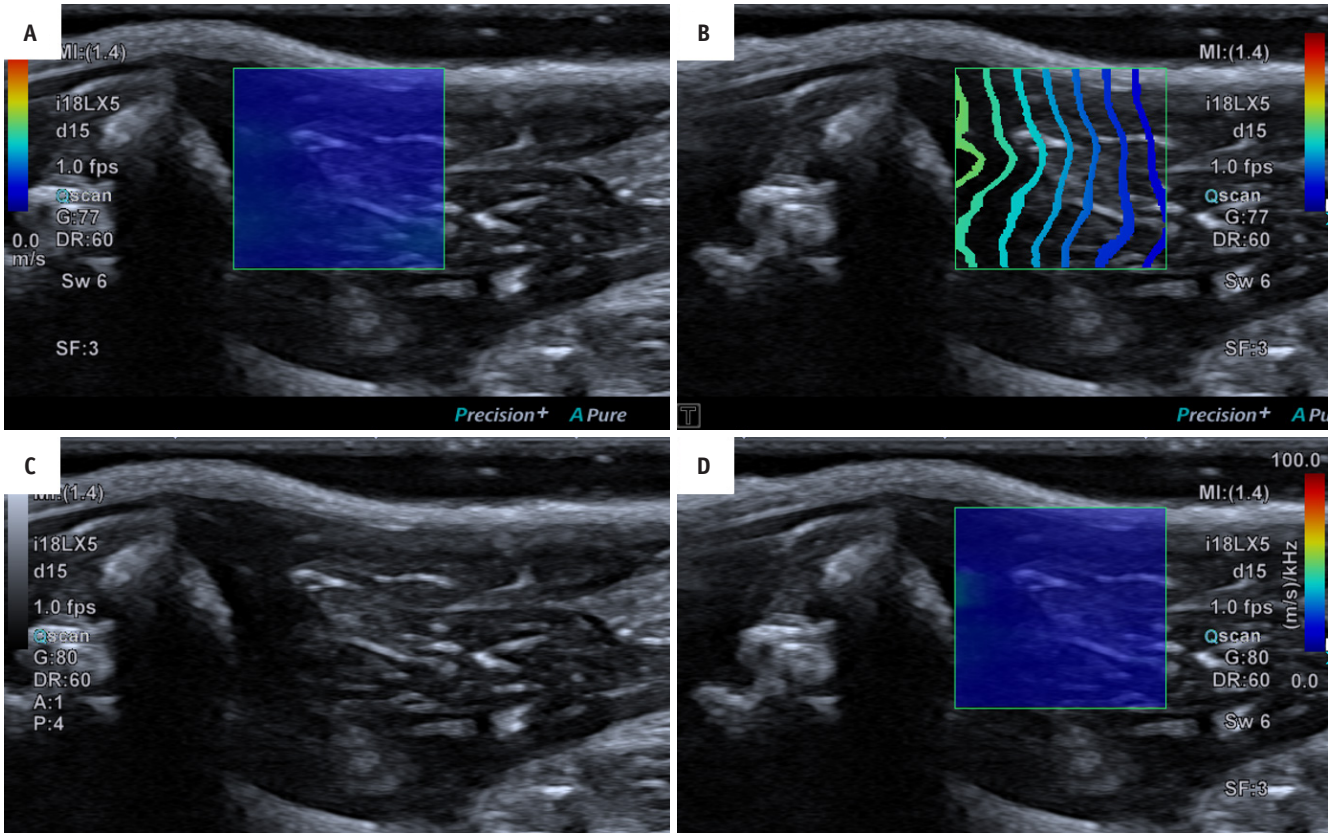

Fig. 1. Quad-view of SWD imaging of the sciatic nerve.
A. Elasticity map. **B.** Propagation map. **C.** B-mode image. **D.** SWD map. SWD = shear wave dispersion

https://doi.org/10.3348/kjr.2021.0603

approximately 1 cm above the bifurcation.

The nerve samples were then evaluated using transmission electron microscopy in both the diabetic and control groups. Briefly, the sciatic nerve specimens were fixed in 3% glutaraldehyde in 0.1 M phosphate buffer (PB) (pH 7.4) at 4°C overnight. Thereafter, they were post-fixed in 1% OsO_4 (Sigma Chemicals Co.) in PB for 2 hours, dehydrated in a graded series of alcohol and propylene oxide (Electron Microscopy Sciences), embedded in resin (Durcupan, ACM-Fluka), and polymerized at 60°C.

Additionally, semithin transections (1 μm) were obtained using an ultramicrotome (MT 6000-XL, RMC) and stained with 1% toluidine blue (Merck) in 1% sodium tetraborate (Ecibra). Semi-thin sections were then observed under a light microscope (x 400) (Olympus BX51) to assess the density of myelinated fibers (number of fibers/mm^2). Afterwards, the resin-embedded tissues were cut into ultrathin sections (70 nm) and double-stained with uranyl acetate and lead citrate. After dehydration with ethanol and acetone, the samples were observed under a transmission electron microscope (x 2550) (Fei Tecnai G2 F20) to assess the thickness of the myelin sheath (μm) and average diameter of the axon (μm). Moreover, all quantitative morphometry data were obtained according to a previously published method [24] using the ImageJ software. In addition, a single investigator blinded to the samples performed morphometric analysis.

Statistical Studies

Statistical analysis was conducted using IBM SPSS Statistics for Windows, Version 22.0; IBM Corp.) and MedCalc, version 18.2.1 (MedCalc Software). The initial set of measurements obtained by operator 1 was used for the main analysis. All data are presented as mean ± standard deviation. In addition, the Anderson–Darling normality test was used to evaluate the data distribution. Differences in the CSA, SWE, and SWD values between the diabetic and control groups were evaluated using Student's *t* test or Welch's *t* test. Statistical significance was set at $p < 0.05$. Moreover, the inter- and intra-observer agreements in measuring SWE and SWD were assessed using intraclass correlation coefficients (ICCs), calculated using the two-way random effects model. The 95% confidence interval (CI) was also determined for each ICC. An ICC of more than 0.80 indicated excellent agreement. Receiver operating characteristic (ROC) curve analysis was performed to determine the performance of CSA, SWD, and SWE in distinguishing the diabetic and control groups. The area under the ROC curve (AUC) was also calculated and compared between the methods using the Hanley–McNeil test.

Table 1. CSA, SWE, and SWD Measurements in the Sciatic Nerves in Both Groups

	CSA (mm^2)	SWE (m/s)	SWD ([m/s]/kHz)
Diabetic group 3m	1.97 ± 0.22	1.75 ± 0.16	8.43 ± 0.90
Control group 3m	1.82 ± 0.24	1.65 ± 0.14	7.25 ± 0.54
p value	0.040	0.020	< 0.001

Data are shown as mean ± standard deviation. CSA = cross-sectional area, SWD = shear wave dispersion imaging, SWE = shear wave elastography, 3m = 3 months

RESULTS

The fasting blood glucose concentration at 3 months of rats in the diabetic group was 25.1 ± 3.1 mmoL/L. The mean values of CSA, nerve viscosity evaluated using SWD imaging, and nerve stiffness evaluated using SWE in the diabetic and control groups are shown in Table 1 and Figure 2. The CSA, viscosity, and stiffness of the nerve in

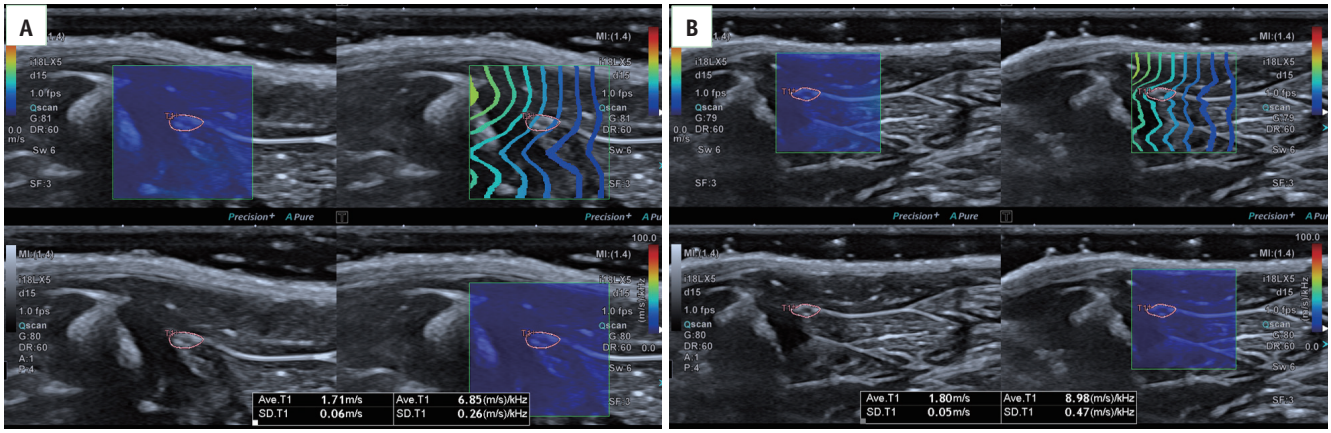

Fig. 2. Shear wave elastography and shear wave dispersion findings of the sciatic nerve in control rat (A) and diabetic rat (B).

https://doi.org/10.3348/kjr.2021.0603

Korean Journal of Radiology
KJR

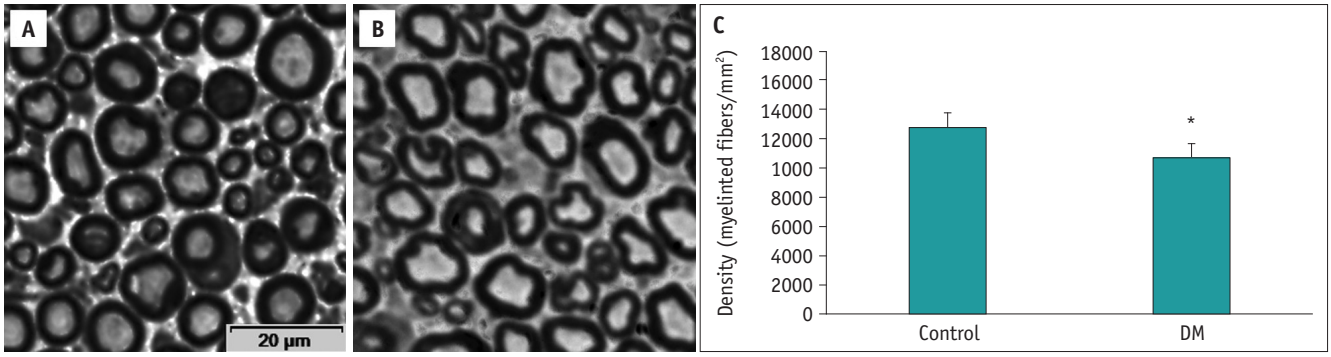

Fig. 3. Myelinated fiber density in the two groups. Toluidine blue-stained semithin sections (1 μm) obtained from the sciatic nerve. **A.** Control group. **B.** Diabetic group (x 400). **C.** Comparison of the density of the myelinated fibers in the two groups. All groups of sciatic nerve morphometric parameters are shown as the density of myelinated fibers. *p < 0.01 compared to control group. DM = diabetes mellitus

the diabetic group were significantly higher than those in the control group (p = 0.040, p < 0.001, and p = 0.020, respectively). There was excellent inter- and intra-observer consistency of the SWE and SWD measurements. In terms of the inter-observer variability for SWE and SWD, the ICC was 0.785 (95% CI, 0.611–0.881) and 0.806 (95% CI, 0.649–0.893), respectively. In terms of the intra-observer variability for SWE and SWD, the ICC was 0.820 (95% CI, 0.675–0.900) and 0.843 (95% CI, 0.716–0.913).

The MNCV of the control group and diabetic group was 64.83 ± 3.66 m/s and 55.17 ± 5.38 m/s, respectively. The MNCV in the diabetic group was significantly lower (p = 0.005).

Analysis of the morphometric data revealed that the diabetic group (10700 ± 944 fibers/mm^2) had a significantly lower density of myelinated fibers than that of the control group (12754 ± 969 fibers/mm^2; p = 0.004), as shown in Figure 3. The results also revealed a considerable level of demyelination (Fig. 4A, B). Notably, the average thickness of the myelin sheath in the diabetic group (0.92 ± 0.38 μm) was smaller than that in the control group (1.15 ± 0.39 μm; p = 0.012) (Fig. 4C). Moreover, although there were atrophic changes in axons, there was no difference in the average diameter of axons between the two groups (p > 0.05), as shown in Figure 4D. The results in Figure 5 also show endothelial cell proliferation, capillary basement membrane thickening, and irregular capillary lumen in the sciatic nerves of diabetic rats.

The AUCs for SWD, SWE, and CSA in distinguishing the diabetic and control groups were 0.876 (95% CI, 0.745–0.955), 0.705 (95% CI, 0.552–0.830) and 0.677 (95% CI, 0.523–0.807), respectively, as shown in Figure 6. The AUC for SWD was significantly greater than that for CSA (p = 0.030) and SWE (p = 0.035).

DISCUSSION

Conventional US can detect morphological changes in the affected peripheral nerve and quantify its CSA [25]. However, the potential value of CSA is limited because of the overlap in CSA between patients with and without DPN. For example, there is a wide range of reported CSA cutoff values (8.9–19.0 mm^2) for the diagnosis of DPN in the tibial nerve [11,26,27].

Microvascular abnormalities, metabolic cascades, end products activated by hyperglycemia, inflammatory processes, oxidative stress, and cellular factors in patients with DM cause decreased blood flow, ischemia, and edema within the nerve [20,28,29], resulting in demyelination and axonal damage, also referred to as DPN [19,30]. The present study showed that in the diabetic group the axons of the sciatic nerve were obviously atrophic, demyelination was observed, and some myelinated fibers displayed Wallerian degeneration. Analysis of the morphometric data also revealed that the density of myelinated fibers was lower in the diabetic group, and diabetic rats had a thinner myelin sheath, consistent with previous findings. This suggests that DM can have a severe effect on nerves [26], which was also demonstrated by the MNCV value. However, there were no differences in the average diameter of axons, possibly because alterations in axons may require a longer period of DPN.

In DPN, the edema in the epineurium and perineurium caused by metabolic disorders associated with DM increases the intra-neural pressure, making the nerve stiffer [31]. With a longer course of DM, focal demyelination and axonal degeneration with a fibrotic response results in the proliferation of scar tissue and increased nerve stiffness [32], which can be measured using SWE. In the present

 https://doi.org/10.3348/kjr.2021.0603

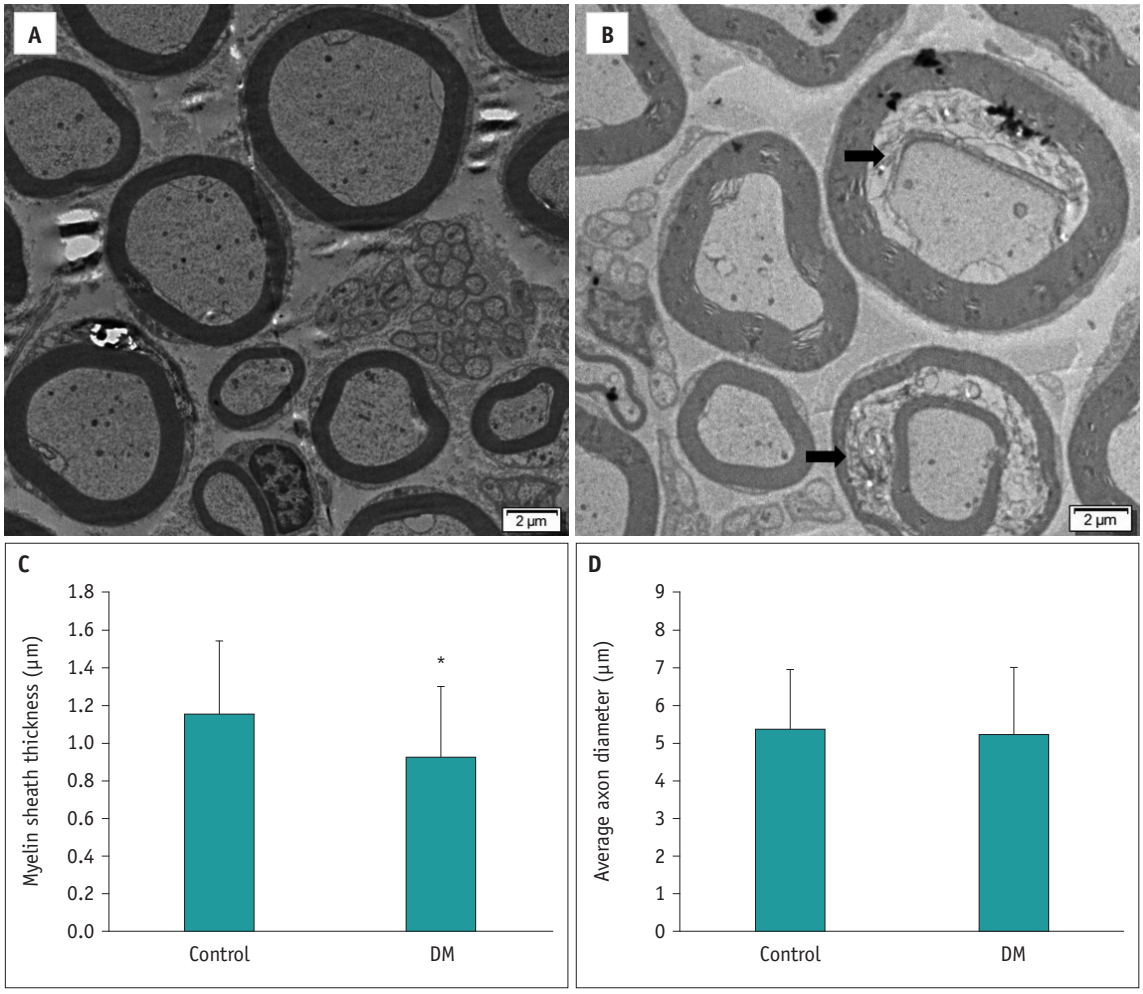

Fig. 4. Pathological changes and morphometric parameters of the sciatic nerve in the study groups. Transmission electron microscopy of the sciatic nerve.
A. Control group. **B.** Diabetic group. Sciatic nerves in diabetic rats; arrows highlights demyelination (x 2550). Morphometric parameters of the sciatic nerve fibers. **C.** Average myelin sheath thickness. **D.** Average axon diameter. All groups of sciatic nerve morphometric parameters are shown as density of myelinated fibers. *p < 0.05 compared to control group. DM = diabetes mellitus

study, the diabetic group had a stiffer sciatic nerve and greater nerve block than those of the control group. These findings were consistent with those previously reported by Dikici et al. [10] and Chen et al. [33], who showed that the tibial nerve in patients with established neuropathy was significantly stiffer than that in healthy controls. Nevertheless, it is noteworthy that nerve tissue has viscoelastic properties [34]. Therefore, both tissue elasticity and viscosity affect shear wave propagation. While several studies have focused on the elastic features of the nerve, little attention has been paid to its viscous properties. Nonetheless, the stiffness of the nerves only reflects a part of the pathological changes. Previous research has shown that inflammation plays an essential role in the pathogenesis of DPN [35,36]. Yan et al. [37] found that patients with type 2 DM and DPN had significantly higher levels of inflammation. Moreover, pro-inflammatory cytokines are associated with significant injury to Schwann cells and neurons in the peripheral nervous system [19,29]. These findings suggest that inflammation during the development of DPN should not be ignored.

It is now well known that both tissue viscosity and elasticity affect the propagation of shear waves. Dispersion is related to the attenuation of shear waves and the frequency dependence of the speed in the viscous component [13]. Therefore, the analysis of the dispersion properties of shear waves can serve as an indirect method for measuring the viscosity. Tissue viscosity has generally been neglected because of the lack of an appropriate method to measure it independently. In recent years,

https://doi.org/10.3348/kjr.2021.0603

Korean Journal of Radiology
KJR

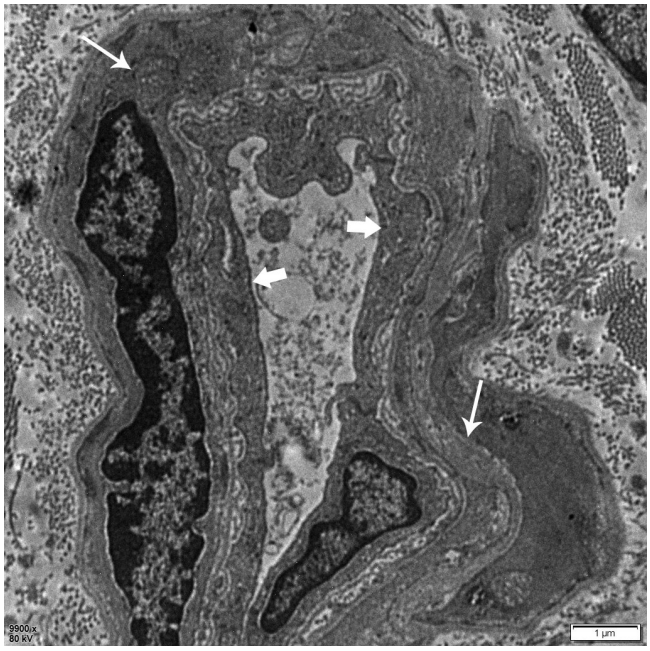

Fig. 5. Transmission electron microscopy of capillaris in diabetic rats. Transmission electron microscopy showed endothelial cell proliferation (thick arrows), thickened capillary basement membrane (thin arrows), and irregular capillary lumen for capillaries supplying the sciatic nerve (x 9900).

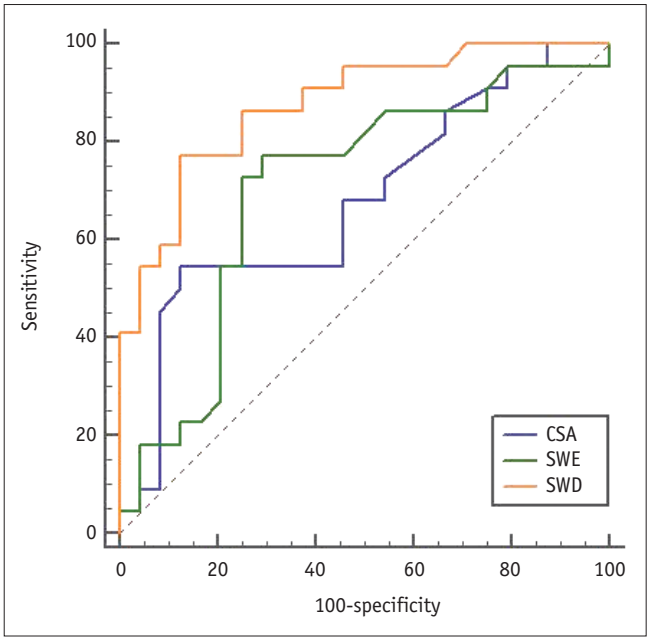

Fig. 6. Receiver operating characteristic curves for distinguishing diabetic and control groups using CSA, SWE, and SWD imaging measurements. CSA = cross-sectional area, SWD = shear wave dispersion, SWE = shear wave elastography

advancements in medical technology have promoted the development of shear wave dispersion imaging, which presents a new platform for the non-invasive evaluation of tissue viscosity. Several studies have not only used SWD in rats but also in human tissues [14-17], and the results showed that viscosity may be related to steatosis, necrosis, and inflammation. Therefore, the present study hypothesized that SWD could evaluate nerve viscosity to determine peripheral nerve damage in rats with DPN. To the best of our knowledge, this is the first study to employ SWD to assess nerve damage in DPN. The results showed that the viscosity of the sciatic nerve (measured using SWD imaging) was markedly higher in diabetic rats than in healthy controls. Histological evaluation revealed that inflammatory changes occurred in the diabetic group. More specifically, there was significantly more microvascular proliferation and inflammation of the perineurium in the diabetic group than in the control group. It is therefore possible that an increase in viscosity in DPN may be related to an increase in microvascular proliferation and inflammation, although this needs to be confirmed through further research.

To investigate whether SWD imaging could accurately diagnose DPN, the study compared the sensitivity and specificity of different features using ROC curve analysis. The findings revealed that the sensitivity and specificity of SWD imaging were higher than those of CSA and SWE. Additionally, the intra- and inter-observer variation analyses of SWD demonstrated high concordance. Overall, these findings suggest that the SWD imaging-based measurement of viscosity might be a sensitive and reproducible method for the diagnosis of DPN.

Consistently, animal models play an important role in preclinical screening of potential new methods. The present findings provide preliminary evidence that SWD can improve the diagnostic accuracy for DPN. Therefore, we believe that SWD can also be applied to the human nerves. We believe that the median nerve, tibial nerve, and sural nerve are potential targets. If confirmed, this may have a potential effect on the future diagnosis of DPN in humans.

While the present study uncovered some insightful findings, it had a number of limitations. First, the study did not quantitatively evaluate inflammatory changes in the sciatic nerves of diabetic rats. Therefore, the quantitative relationship between viscosity measured using SWD imaging and inflammatory changes in DPN has not been clarified. Second, the value of SWD imaging for grading DPN was not elaborated in this study. Third, the SWE and SWD measurements were obtained from a transverse section of the sciatic nerve, and longitudinal sections

 https://doi.org/10.3348/kjr.2021.0603

were not routinely obtained. This is because the ROI could not be fixed to a uniform size over the epineurium in a longitudinal section, which may affect the accuracy of the measurement.

In conclusion, this study showed that the viscosity of the sciatic nerve measured using SWD imaging was significantly higher in the DM group than in the control group. In addition, SWD could better distinguishing the diabetic and control groups than SWE or CSA. Therefore, SWD may be a promising method for evaluating DPN.

Availability of Data and Material

The datasets generated or analyzed during the study are available from the corresponding author on reasonable request.

Conflicts of Interest

The authors have no potential conflicts of interest to disclose.

Author Contributions

Conceptualization: Fang Liu, Jiaan Zhu. Data curation: Feifei Liu, Diancheng Li, Yuwei Xin, Wenxue Li. Formal analysis: Feifei Liu, Diancheng Li. Funding acquisition: Fang Liu, Jiaan Zhu. Investigation: Feifei Liu, Diancheng Li, Yuwei Xin. Methodology: Feifei Liu, Diancheng Li, Yuwei Xin, Fang Liu, Wenxue Li. Project administration: Fang Liu, Jiaan Zhu. Resources: Feifei Liu, Diancheng Li, Yuwei Xin. Supervision: Fang Liu, Wenxue Li, Jiaan Zhu. Validation: Feifei Liu, Diancheng Li, Yuwei Xin. Writing—original draft: Feifei Liu, Diancheng Li. Writing—review & editing: all authors.

ORCID iDs

Feifei Liu
https://orcid.org/0000-0003-2948-4320
Diancheng Li
https://orcid.org/0000-0001-8223-2574
Yuwei Xin
https://orcid.org/0000-0002-2209-7718
Fang Liu
https://orcid.org/0000-0002-9683-184X
Wenxue Li
https://orcid.org/0000-0001-7237-7788
Jiaan Zhu
https://orcid.org/0000-0001-8700-639X

Funding Statement

This study was supported by the National Natural Science Foundation of China (No. 82071930, 81571684, and 81701712).

Acknowledgments

We are grateful to Dr. Yusong Yuan for his assistance with electrophysiological examinations.

REFERENCES

1. Pop-Busui R, Boulton AJ, Feldman EL, Bril V, Freeman R, Malik RA, et al. Diabetic neuropathy: a position statement by the American Diabetes Association. *Diabetes Care* 2017;40:136-154
2. Tesfaye S, Boulton AJ, Dyck PJ, Freeman R, Horowitz M, Kempler P, et al. Diabetic neuropathies: update on definitions, diagnostic criteria, estimation of severity, and treatments. *Diabetes Care* 2010;33:2285-2293
3. Edmonds M, Manu C, Vas P. The current burden of diabetic foot disease. *J Clin Orthop Trauma* 2021;17:88-93
4. Hicks CW, Selvin E. Epidemiology of peripheral neuropathy and lower extremity disease in diabetes. *Curr Diab Rep* 2019;19:86
5. Dyck PJ, Overland CJ, Low PA, Litchy WJ, Davies JL, Dyck PJ, et al. Signs and symptoms versus nerve conduction studies to diagnose diabetic sensorimotor polyneuropathy: Cl vs. NPhys trial. *Muscle Nerve* 2010;42:157-164
6. Singleton JR, Bixby B, Russell JW, Feldman EL, Peltier A, Goldstein J, et al. The Utah Early Neuropathy Scale: a sensitive clinical scale for early sensory predominant neuropathy. *J Peripher Nerv Syst* 2008;13:218-227
7. Bae JS, Kim BJ. Subclinical diabetic neuropathy with normal conventional electrophysiological study. *J Neurol* 2007;254:53-59
8. Radziwill AJ, Steck AJ, Renaud S, Fuhr P. Distal motor latency and residual latency as sensitive markers of anti-MAG polyneuropathy. *J Neurol* 2003;250:962-966
9. Li D, Zhu J, Liu F, Li B, Liu F, Li W. A quantitative evaluation of sciatic nerve stiffness after compression by shear wave elastography in diabetic rats. *Ann Transl Med* 2020;8:682
10. Dikici AS, Ustabasioglu FE, Delil S, Nalbantoglu M, Korkmaz B, Bakan S, et al. Evaluation of the tibial nerve with shear-wave elastography: a potential sonographic method for the diagnosis of diabetic peripheral neuropathy. *Radiology* 2017;282:494-501
11. He Y, Xiang X, Zhu BH, Qiu L. Shear wave elastography evaluation of the median and tibial nerve in diabetic peripheral neuropathy. *Quant Imaging Med Surg* 2019;9:273-282
12. Jiang W, Huang S, Teng H, Wang P, Wu M, Zhou X, et al. Diagnostic performance of two-dimensional shear wave elastography for evaluating tibial nerve stiffness in patients

https://doi.org/10.3348/kjr.2021.0603

with diabetic peripheral neuropathy. *Eur Radiol* 2019;29:2167-2174
13. Chen S, Urban MW, Pislaru C, Kinnick R, Greenleaf JF. Liver elasticity and viscosity quantification using shearwave dispersion ultrasound vibrometry (SDUV). *Annu Int Conf IEEE Eng Med Biol Soc* 2009;2009:2252-2255
14. Lee DH, Lee JY, Bae JS, Yi NJ, Lee KW, Suh KS, et al. Shear-wave dispersion slope from US shear-wave elastography: detection of allograft damage after liver transplantation. *Radiology* 2019;293:327-333
15. Suzuki H, Kawashima H, Ohno E, Ishikawa T, Hashimoto S, Nakamura M, et al. What is the role of measuring shear wave dispersion using shear wave elastography in pancreatic parenchyma? *J Med Ultrason (2001)* 2020;47:575-581
16. Sugimoto K, Moriyasu F, Oshiro H, Takeuchi H, Yoshimasu Y, Kasai Y, et al. Viscoelasticity measurement in rat livers using shear-wave US elastography. *Ultrasound Med Biol* 2018;44:2018-2024
17. Sugimoto K, Moriyasu F, Oshiro H, Takeuchi H, Yoshimasu Y, Kasai Y, et al. Clinical utilization of shear wave dispersion imaging in diffuse liver disease. *Ultrasonography* 2020;39:3-10
18. Chaudhuri O. Viscoelastic hydrogels for 3D cell culture. *Biomater Sci* 2017;5:1480-1490
19. Kaul K, Hodgkinson A, Tarr JM, Kohner EM, Chibber R. Is inflammation a common retinal-renal-nerve pathogenic link in diabetes? *Curr Diabetes Rev* 2010;6:294-303
20. Jahantigh Akbari N, Hosseinifar M, Naimi SS, Mikaili S, Rahbar S. The efficacy of physiotherapy interventions in mitigating the symptoms and complications of diabetic peripheral neuropathy: a systematic review. *J Diabetes Metab Disord* 2020;19:1995-2004
21. Yagihashi S, Mizukami H, Sugimoto K. Mechanism of diabetic neuropathy: where are we now and where to go? *J Diabetes Investig* 2011;2:18-32
22. Reed MJ, Meszaros K, Entes LJ, Claypool MD, Pinkett JG, Gadbois TM, et al. A new rat model of type 2 diabetes: the fat-fed, streptozotocin-treated rat. *Metabolism* 2000;49:1390-1394
23. Junod A, Lambert AE, Stauffacher W, Renold AE. Diabetogenic action of streptozotocin: relationship of dose to metabolic response. *J Clin Invest* 1969;48:2129-2139
24. Ilha J, Araujo RT, Malysz T, Hermel EE, Rigon P, Xavier LL, et al. Endurance and resistance exercise training programs elicit specific effects on sciatic nerve regeneration after experimental traumatic lesion in rats. *Neurorehabil Neural Repair* 2008;22:355-366
25. Moran L, Royuela A, de Vargas AP, Lopez A, Cepeda Y, Martinelli G. Carpal tunnel syndrome: diagnostic usefulness of ultrasound measurement of the median nerve area and quantitative elastographic measurement of the median nerve stiffness. *J Ultrasound Med* 2020;39:331-339
26. Watanabe T, Ito H, Sekine A, Katano Y, Nishimura T, Kato Y, et al. Sonographic evaluation of the peripheral nerve in diabetic patients: the relationship between nerve conduction studies, echo intensity, and cross-sectional area. *J Ultrasound Med* 2010;29:697-708
27. Riazi S, Bril V, Perkins BA, Abbas S, Chan VW, Ngo M, et al. Can ultrasound of the tibial nerve detect diabetic peripheral neuropathy? A cross-sectional study. *Diabetes Care* 2012;35:2575-2579
28. Lupachyk S, Watcho P, Hasanova N, Julius U, Obrosova IG. Triglyceride, nonesterified fatty acids, and prediabetic neuropathy: role for oxidative-nitrosative stress. *Free Radic Biol Med* 2012;52:1255-1263
29. Yoon H, Thakur V, Isham D, Fayad M, Chattopadhyay M. Moderate exercise training attenuates inflammatory mediators in DRG of Type 1 diabetic rats. *Exp Neurol* 2015;267:107-114
30. Malik RA, Veves A, Walker D, Siddique I, Lye RH, Schady W, et al. Sural nerve fibre pathology in diabetic patients with mild neuropathy: relationship to pain, quantitative sensory testing and peripheral nerve electrophysiology. *Acta Neuropathol* 2001;101:367-374
31. Clements RS Jr. Diabetic neuropathy--new concepts of its etiology. *Diabetes* 1979;28:604-611
32. Widgerow AD. Cellular/extracellular matrix cross-talk in scar evolution and control. *Wound Repair Regen* 2011;19:117-133
33. Chen R, Wang XL, Xue WL, Sun JW, Dong XY, Jiang ZP, et al. Application value of conventional ultrasound and real-time shear wave elastography in patients with type 2 diabetic polyneuropathy. *Eur J Radiol* 2020;126:108965
34. Chang CT, Chen YH, Lin CC, Ju MS. Finite element modeling of hyper-viscoelasticity of peripheral nerve ultrastructures. *J Biomech* 2015;48:1982-1987
35. Baum P, Kosacka J, Estrela-Lopis I, Woidt K, Serke H, Paeschke S, et al. The role of nerve inflammation and exogenous iron load in experimental peripheral diabetic neuropathy (PDN). *Metabolism* 2016;65:391-405
36. Kosacka J, Woidt K, Toyka KV, Paeschke S, Klöting N, Bechmann I, et al. The role of dietary non-heme iron load and peripheral nerve inflammation in the development of peripheral neuropathy (PN) in obese non-diabetic leptin-deficient ob/ob mice. *Neurol Res* 2019;41:341-353
37. Yan P, Zhang Z, Miao Y, Xu Y, Zhu J, Wan Q. Physiological serum total bilirubin concentrations were inversely associated with diabetic peripheral neuropathy in Chinese patients with type 2 diabetes: a cross-sectional study. *Diabetol Metab Syndr* 2019;11:100

https://doi.org/10.3348/kjr.2021.0603